ASIAN JOURNAL OF CIVIL ENGINEERING (BUILDING AND HOUSING) VOL. 8, NO. 3 (2007)
PAGES 247-265

MOMENT CURVATURE OF REINFORCED CONCRETE BEAMS USING VARIOUS CONFINEMENT MODELS AND EXPERIMENTAL VALIDATION

M. Srikanth, G. Rajesh Kumar* and S. Giri
Department of Civil Engineering, National Institute of Technology, Waragal-506 004, India

ABSTRACT

This paper presents a procedure for finding the analytical Moment Curvature behaviour of statically determinate reinforced concrete beams, taking into consideration, the confinement offered by shear reinforcement to concrete in compression zone. Six selected confinement models reported in literature in the last decade are used as a stress block for confined concrete for generating the complete analytical Moment Curvature behaviour. The Moment Curvature behaviour obtained using the selected confinement models are compared with experimental results. In general it is observed that the results obtained from the selected models were close to the experimental values. However, it is observed that the analytical values obtained using Mendis and Cusson model are closer to the experimental results when compared to that obtained using the other models.

Keywords: stress, strain, moment, curvature, confinement

1. INTRODUCTION

The most fundamental requirement in predicting the Moment Curvature behaviour of a flexural member is the knowledge of the behaviour of its constituents. With the increasing use of higher-grade concretes, the ductility of which is significantly less than normal concrete, it is essential to confine the concrete. In a flexure member the shear reinforcement also confines the concrete in the compression zone. Hence, to predict the Moment Curvature behaviour of a flexural member, the stress–strain behaviour of confined concrete in axial compression is essential. With the development of performance-based design methods, there is an increasing need for simplified but reliable analytical tools capable of predicting the flexural behaviour of reinforced concrete members. Design offices will be faced more and more with the need of predicting the deformation capacity of concrete members. A general approach to account for confinement of concrete and predicting the flexural behaviour of concrete member is needed. In light of the above six confinement models proposed by various authors in the last decade (1995-2005) were selected and used as stress block for

* Email-address of the corresponding author: garjesri@yahoo.co.in

compression concrete in an RC beam for generating analytical M-ϕ behaviour. The analytical values obtained using various models were compared with experimental results.

2. CONFINEMENT MODELS

The confinement models used for predicting the Moment Curvature behaviour of RC beams are listed below and the mathematical expressions of the selected models are given in Table 1.

- Daniel Cusson and Patrick Paultre (Cusson model) [2]
- G. Rajesh Kumar and A. Kamasundara Rao (GRK model) [5]
- Salim Razvi and Murat Saatciglu (Razvi model) [11]
- P.Mendis, R. Pendyala and S. Setunge (Mendis model) [7]
- Frederic Legeron and Patrick Paultre (Legeron model) [6]
- Weena P. Lokunge, J.G. Sanjayan and Sujeeva Setunge (Weena model) [13]

Table 1. Mathematical expressions for various models

Model	Expression for ascending branch	Expression for descending branch
Cusson et al [2]	$f_c = f_{cc}\left[\dfrac{k\left(\varepsilon_c/\varepsilon_{cc}\right)}{k-1+\left(\varepsilon_c/\varepsilon_{cc}\right)^k}\right]$	$f_c = f_{cc}e^{[k_1(\varepsilon_c-\varepsilon_{cc})^{k_2}]}$
GRK et al [5]	$f = \dfrac{A\varepsilon + D\varepsilon^2}{1.0 + B\varepsilon + C\varepsilon^2}$ $A = 2.878\left(f_{cb}/\varepsilon_{cb}\right), B = 0.878\left(1/\varepsilon_{cb}\right)$ $C = -0.439\left(1/\varepsilon_{cb}^2\right), D = -1.439\left(f_{cb}/\varepsilon_{cb}^2\right)$	Same for ascending and descending branch $\dfrac{f_{cb}}{f_c^{'}} = 1.607\,C_i^{0.107}$; $\dfrac{\varepsilon_{cb}}{\varepsilon_c^{'}} = 5.13C_i^{0.286}$ $C_i = (P_b - P_{bb})\dfrac{f_v}{f_c^{'}}\sqrt{\dfrac{b}{s}}$
Razvi et al [11]	$f_c = \dfrac{f_{cc}^{'}\left(\dfrac{\varepsilon_c}{\varepsilon_1}\right)r}{r-1+\left(\dfrac{\varepsilon_c}{\varepsilon_1}\right)^r}$	$\varepsilon_{85} = 260k_3\rho_c\varepsilon_1[1+0.5k_2(k_4-1)]+\varepsilon_{085}$ (linear from peak to the 0.85 of peak stress and 0.2 of peak stress in descending portion after which it is residual stress)
Mendis et al [7]	$f = Kf_c^{'}\left[\dfrac{2\varepsilon}{\varepsilon_{cc}} - \left(\dfrac{\varepsilon}{\varepsilon_{cc}}\right)^2\right]$	$f = Kf_c^{'}[1-Z_m(\varepsilon-\varepsilon_{cc})] \geq f_{res}$
Legeron et al [6]	$f_{cc} = f_{cc}^{'}\left[\dfrac{k\left(\varepsilon_{cc}/\varepsilon_{cc}^{'}\right)}{k-1+\left(\varepsilon_{cc}/\varepsilon_{cc}^{'}\right)^k}\right]$	$f_{cc} = f_{cc}^{'}e^{[k_1(\varepsilon_{cc}-\varepsilon_{cc}^{'})^{k_2}]}$
Weena et al [13]	$\sigma_1 = 2\tau_{mp}\left(1-e^{-c\left(\frac{\varepsilon_1+\varepsilon_2}{2\gamma_{mp}}\right)}\right)+f_l$	$\sigma_1 = 2\tau_{mp}\left(e^{d\left(\frac{\varepsilon_1+\varepsilon_2}{2\gamma_{mp}}\right)^2}-d\right)+f_l$

3. ANALYTICAL MOMENT CURVATURE RELATIONSHIP M-ϕ

In deriving the expressions of the moments and curvatures for concrete section confined with rectilinear ties, the following assumptions were made:

a) The stress-strain relationship proposed in a selected model is taken as a stress block.
b) The tensile strength of concrete is neglected.
c) The variation of strain across the section is linear upto failure.
d) Idealised stress-strain relation for the tension and compression steel was used
e) The steel is perfectly bonded.
f) An imaginary leg of stirrup is considered at neutral axis to simulate the triaxial state of stress in compression concrete.

In addition to above assumptions, the three basic relationship viz., (i) Equilibrium of forces, (ii) compatibility of strains and (iii) Stress-strain relationship of the materials have to be satisfied.

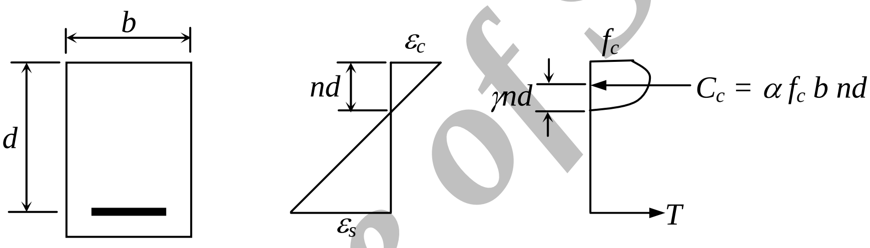

Figure 1. Section strain and stress distribution.

where,
b = width of the beam, d = effective depth of the tension steel, nd = neutral axis depth, f_c=stress in extreme compression fiber, ε_c = extreme compression fiber strain, ε_s = steel strain and γ & α are reduction factors for distance between CG from neutral axis and area under stress-strain curve respectively.

We have, from figure1,
Compressive force (C_c)

$$C_c = \frac{b.nd}{\varepsilon_c}\int_0^{\varepsilon_c} f d\varepsilon \qquad (1)$$

and, moment of compressive force (C_c) about neutral axis (M_c)

$$M_c = b\left(\frac{nd}{\varepsilon_c}\right)^2 . \int_0^{\varepsilon_c} f.\varepsilon.d\varepsilon \qquad (2)$$

Thus, in equation (1) and (2), if the area under concrete stress-strain curve and moment of area under the stress-strain curve is known the compressive force (C_c) and its moment about neutral axis (M_c) can be evaluated.

Step-by-Step Calculation Procedure

For obtaining the complete moment–curvature relationship for any cross-section, discrete values of concrete strains (ε_c) were selected such that even distributions of points on the plot, both before and after the maximum were obtained. The procedure used in computation is given below:

1. The extreme fiber concrete compressive strain (ε_c) was assumed. In present investigation the values of ε_c was in the range of 0.0001 to the failure strain (ie 0.01).
2. The neutral axis depth, *nd*, was assumed initially as 0.5 times the effective depth (i.e. 0.5d)
3. For this value of neutral axis depth, the compressive force in the concrete, 'C_c' was calculated from the respective stress-strain model.
4. The strain in tension and compression steel was calculated, based on the strain compatibility.
5. Based on the strains in tension steels. The corresponding stresses were taken from stress-stress curve of steel.
6. The total tensile force (T) in tensile steel was calculated.
7. Same process was repeated for compressive steel to calculate the compressive force (C_s) in compression steel.
8. The total compressive force C acting in the section was calculated as $C = C_c + C_s$.
9. If $C = T$, then the assumed value of neutral axis depth (*nd*) was correct, and the moment (M) and the corresponding curvature (ϕ) was calculated. Otherwise, the neutral axis depth was modified until the condition $C = T$ was achieved.

Now, the total moment about the N.A. was given by;

$M = M_t$ (moment of force in tensile steel about the neutral axis)+ M_c(moment of compressive force in concrete about the neutral axis) +M_{cs}(moment of force in compression steel about the neutral axis) and the corresponding curvature (ϕ) was given by; $\phi = \frac{\varepsilon_c}{nd}$.

4. EXPERIMENTAL PROGRAMME

The analytical moment curvature relation obtained using various models were compared with experimental results. The experimental programme consisted of casting six beams of three different concrete strengths. For each concrete strength, one under-reinforced (U1, U2, U3) and one over reinforced (O1, O2, O3) beams was cast. The details of the beams are given in Table 2. The balanced reinforcement required for a particular strength of concrete was arrived based on the stress–strain curve as suggested by IS 456: 2000 [15], without considering the partial safety factors.

Table 2. Details of beams used for experimentation.

Beam	f_{ck} (MPa)	Balanced steel (%)	Tension steel	Provided steel (%)
U1	42.54	2.97	2-12 mm	0.882
O1	47.34	3.23	2-12 mm + 2-20 mm	3.411
U2	39.65	2.80	2-16 mm	1.586
O2	39.01	2.77	2-16 mm + 2-20 mm	4.114
U3	47.92	3.26	2-16 mm	1.586
O3	44.23	3.06	2-16 mm + 2-20 mm	4.114

Note: 1. 2- 4 mm GI wire were used as hanger bar (Compression steel) in all the beams

2. 8 mm bar was used as stirrups in all the beams with spacing of 125 mm c-c in under reinforced beams(U) and 100 mm c-c in over reinforced beams(O)

The size of the beam was 150mm × 200mm × 2100mm, with effective span of 1800mm. 53 grade OPC cement conforming to IS 12269:1987 [16], Zone II sand and 20 mm well graded coarse aggregate confirming to IS-383: 1970 [14] was used for casting all the beams. Potable water was used for mixing as well as curing of concrete. The yield strength of 8mm, 12 mm, 16 mm and 20 mm bars were 503.55 MPa, 400.85 MPa, 409.55 MPa, 473.37 MPa respectively. 8mm dia steel was used for stirrups. The spacing of 125 mm and 100 mm was provided to prevent the shear failure of beams.

The beams thus cast were tested under two-point symmetrical loading, with constant moment zone of 300 mm, in order to ensure the flexural failure. The schematic sketch of test setup is given in figure 2.

4.1 Comparison of analytical behaviour with the experimental behaviour

The predicted moment curvature obtained using the selected confinement models were compared with the experimental moment curvature data both graphically and numerically. The Figures 3 and 4 show graphical comparison of the moment curvature behaviour. For the numerical comparison three significant points were chosen namely; ultimate moment and corresponding curvature (M_u and ϕ_u), moment and corresponding curvature at 85 % of the ultimate moment in ascending portion ($M_{0.85,a}$ and $\phi_{0.85,a}$) and the moment and corresponding curvature at 85% of the ultimate moment in descending portion ($M_{0.85,d}$ and $\phi_{0.85,d}$). The experimental strain in concrete (ε_c) and steel (ε_s) at the above mentioned points and their corresponding moment and curvature values were taken as the comparison criteria. The analytical moments and curvatures corresponding to the experimental strains in concrete and steel were considered for comparison. In general, it was noticed that strain in steel was the governing criteria in under-reinforced beam while it was the concrete strain in over-reinforced beam. The Table 3 shows the experimental moment, corresponding curvature, strain in steel and concrete at ultimate moment, 85 % of the ultimate moment in ascending portion and 85 % of the ultimate moment in descending portion.

The experimental and analytical values thus obtained were used for the numerical comparison. The ratio of analytical/experimental values was calculated at all the significant points. The average of analytical to experimental ratios and mean error in prediction was taken for the comparison. The table 4, 5 and 6 shows the comparison of moment and corresponding curvature at the three significant points all the models. The average and mean error in prediction is listed at the bottom of each table.

5. DISCUSSION

i) Ultimate Moment (M_u)

The table 4 shows the comparison of ultimate moment and corresponding curvature for all the models under consideration. The selected models showed a mixed result while predicting the ultimate moment. The Legeron, GRK, Mendis and Weena model slightly overestimated the ultimate moment while the Cusson and Mendis model underestimated the value. However, the average ratios were close to 1.0. The prediction of ultimate moment using Cusson's model had the least mean error of 3.91%.

ii) Curvature corresponding to the ultimate moment (ϕ_u)

All the models under consideration underestimated the curvature corresponding to the ultimate moment. The variation of mean error in predicting the curvature corresponding to the ultimate moment was slightly high but was within the limit of 15%. The prediction made by Mendis model regarding the curvature is better than the other models under consideration.

iii) 85% of Ultimate Moment in ascending portion ($M_{0.85,a}$)

The table 5 shows the comparison of 85% of ultimate moment and corresponding curvature in ascending portion for all the models under consideration. The predictions made by most of the selected models were on the higher side. But, the GRK model slightly underestimated the 85% of ultimate moment in ascending portion and also had higher value of mean error. The mean error in prediction of 85% of ultimate moment in ascending portion by Legeron, Cusson and Razvi model were almost same and was around 10%. With a mean error of 9.89% the prediction using Mendis model was fairly good.

iv) Curvature corresponding to 85% of Ultimate Moment in ascending portion ($\phi_{0.85,a}$)

In general, all the selected models underestimated the value of curvature corresponding to 85% of ultimate moment in ascending portion. Except the GRK model, all the other selected models were good enough to predict the values with less mean error around 10%. The mean error was more in GRK model for the curvature corresponding to 85% of ultimate moment in ascending portion. The Legeron, Cusson and Weena model had approximately equal value of mean error. However, the prediction made by Cusson model for curvature corresponding to 85% of ultimate moment in ascending portion was better.

v) 85% of Ultimate Moment in descending portion ($M_{0.85,d}$ *)*

The table 6 shows the comparison of 85% of ultimate moment and corresponding curvature in descending portion for all the models under consideration. In general, all the selected models overestimated the value, but while the Cusson model slightly underestimated it. The GRK model highly overestimated the value with the highest mean error of 27.63%. The prediction made by Weena and Razvi model were slightly on the higher side with a mean error around 14% but was well within the acceptable limit of 15%. The prediction made by Legeron and Cusson model was similar with approximately same value of mean error and average value. But, the values of 85% of ultimate moment descending portion estimated by Cusson model were closer to the test results.

vi) Curvature corresponding to 85% of Ultimate Moment in descending portion ($\phi_{0.85,d}$ *)*

The selected models showed a mixed result while estimating the value of curvature corresponding to the 85% of ultimate moment descending portion. The Legeron, Cusson and Razvi models overestimated the value and had a higher value of mean error around 17%. When compared to the other models, the predictions made by Mendis and Weena models were better with approximately same value of mean error around 12%. However, the prediction of the curvature corresponding to the 85% of ultimate moment descending portion made by Mendis model was found to be better when compared to the other models.

6. CONCLUSIONS

A procedure for obtaining analytical moment-curvature behaviour taking into consideration the confinement effect due to shear reinforcement was developed. Six different confinement models published in literature in the last decade were taken as a stress block for compression concrete for generating an analytical moment-curvature curve. The analytical values obtained were validated with experimental results. The analytical to experimental ratio and mean error in prediction was used for the comparison. In general, the analytical results obtained using selected models were closer to the experimental results. However, it was observed that the analytical values obtained using Mendis and Cusson model were closer to the experimental results when compared to that obtained using the other models.

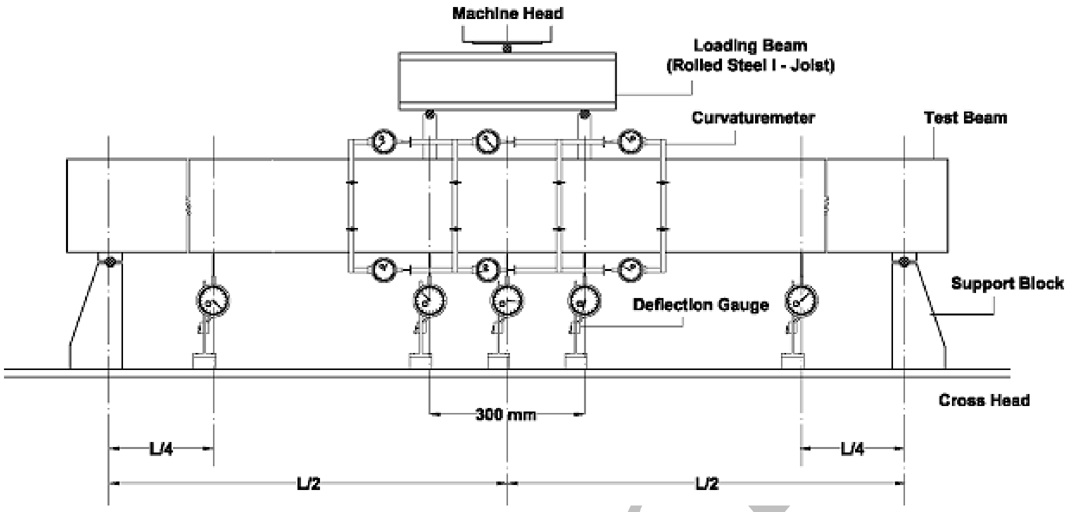

Figure 2. Schematic sketch of the test setup

Table 3. Experimental Moment, Corresponding Curvature and Strain in Concrete and Steel at Three Significant Points

Beam	Ultimate				85 % of Ultimate in ascending portion				85 % of Ultimate in descending portion			
	M_u (kN-m)	ϕ_u ($\times 10^{-6}$)	ε_c ($\times 10^{-6}$)	ε_s ($\times 10^{-6}$)	$M_{0.85,a}$ (kN-m)	$\phi_{0.85,a}$ ($\times 10^{-6}$)	ε_c ($\times 10^{-6}$)	ε_s ($\times 10^{-6}$)	$M_{0.85,d}$ (kN-m)	$\phi_{0.85,d}$ ($\times 10^{-6}$)	ε_c ($\times 10^{-6}$)	ε_s ($\times 10^{-6}$)
U1	16.55	131.86	1961.43	20317.59	14.01	24.97	786.62	3432.23	15.61	203.96	3889.94	30571.72
O1	39.37	45.79	4237.45	3183.62	33.09	24.67	2028.00	1969.85	36.03	88.70	7910.36	6465.20
U2	24.29	125.03	4083.38	16417.86	20.95	24.79	1476.31	2587.95	20.82	273.60	15949.33	28912.46
O2	41.90	47.77	4222.78	3519.15	35.76	23.46	2019.94	1781.64	35.63	125.05	13992.48	6274.33
U3	24.55	87.18	3489.32	10893.20	20.82	20.71	1192.26	2224.61	22.55	142.88	8567.40	15003.39
O3	47.11	34.14	2874.66	3441.44	40.30	23.31	1887.73	2425.15	40.17	57.67	6951.23	3717.48

Table 4. Comparison of ultimate moment and corresponding curvature

Beam	Experimental		Cusson		GRK		Razvi		Mendis		Legeron		Weena	
	M_u (kN-m)	ϕ_u ($\times 10^{-6}$)	$\frac{M_{u,ana}}{M_{u,exp}}$	$\frac{\phi_{u,ana}}{\phi_{u,exp}}$	$\frac{M_{u,ana}}{M_{u,exp}}$	$\frac{\phi_{u,ana}}{\phi_{u,exp}}$	$\frac{M_{u,ana}}{M_{u,exp}}$	$\frac{\phi_{u,ana}}{\phi_{u,exp}}$	$\frac{M_{u,ana}}{M_{u,exp}}$	$\frac{\phi_{u,ana}}{\phi_{u,exp}}$	$\frac{M_{u,ana}}{M_{u,exp}}$	$\frac{\phi_{u,ana}}{\phi_{u,exp}}$	$\frac{M_{u,ana}}{M_{u,exp}}$	$\frac{\phi_{u,ana}}{\phi_{u,exp}}$
U1	16.55	149.15	0.962	1.008	1.011	0.973	1.025	0.952	0.953	0.944	0.966	1.000	1.005	0.943
O1	39.37	45.79	1.098	0.966	1.167	0.946	1.127	1.040	0.940	1.028	1.165	1.011	1.189	1.084
U2	24.29	125.03	0.976	0.564	1.099	1.063	1.018	1.042	0.992	1.044	0.990	0.590	1.047	0.726
O2	41.90	47.77	0.977	0.816	1.033	0.795	1.063	0.847	0.791	0.852	1.040	0.843	1.077	0.872
U3	24.55	87.18	1.000	1.058	1.060	0.978	1.066	0.955	0.976	0.989	1.020	1.022	1.057	0.944
O3	47.11	37.06	0.948	0.767	0.793	0.691	0.935	0.735	0.962	0.772	0.962	0.772	0.975	0.801
		Average	0.993	0.863	1.027	0.908	1.039	0.928	0.936	0.938	1.024	0.873	1.058	0.895
		Mean error	3.91%	15.87%	9.62%	11.34%	6.07%	9.91%	6.44%	8.58%	5.09%	13.81%	6.66%	13.32%

Table 5. Comparison of 85% of ultimate moment and corresponding curvature in ascending portion

Beam	Experimental		Cusson		GRK		Razvi		Mendis		Legeron		Weena	
	85% of Ultimate Moment and Corresponding Curvature in ascending portion (ana./exp.)													
	$M_{0.85,a}$ (kN-m)	$\phi_{0.85,a}$ ($\times 10^{-6}$)	$\frac{M_{0.85a,ana}}{M_{0.85a,\exp}}$	$\frac{\phi_{0.85a,ana}}{\phi_{0.85a,\exp}}$	$\frac{M_{0.85a,ana}}{M_{0.85a,\exp}}$	$\frac{\phi_{0.85a,ana}}{\phi_{0.85a,\exp}}$	$\frac{M_{0.85a,ana}}{M_{0.85a,\exp}}$	$\frac{\phi_{0.85a,ana}}{\phi_{0.85a,\exp}}$	$\frac{M_{0.85a,ana}}{M_{0.85a,\exp}}$	$\frac{\phi_{0.85a,ana}}{\phi_{0.85a,\exp}}$	$\frac{M_{0.85a,ana}}{M_{0.85a,\exp}}$	$\frac{\phi_{0.85a,ana}}{\phi_{0.85a,\exp}}$	$\frac{M_{0.85a,ana}}{M_{0.85a,\exp}}$	$\frac{\phi_{0.85a,ana}}{\phi_{0.85a,\exp}}$
U1	14.01	24.97	1.040	1.058	1.020	1.219	1.038	1.170	1.034	1.081	1.040	1.058	1.050	1.015
O1	33.09	24.67	1.284	0.886	0.917	0.780	1.142	0.844	1.210	0.863	1.269	0.882	1.324	0.936
U2	20.95	24.79	1.132	0.968	1.109	1.127	1.127	1.032	1.125	0.975	1.132	0.968	1.153	1.146
O2	35.76	23.46	1.055	0.873	0.749	0.779	0.939	0.837	1.007	0.856	1.040	0.869	1.091	0.891
U3	20.82	20.71	1.151	1.052	1.120	1.185	1.132	1.003	1.141	1.058	1.151	1.052	1.161	0.918
O3	40.30	23.31	0.981	0.862	0.688	0.762	0.865	0.822	0.923	0.841	0.967	0.858	1.034	0.887
		Average	1.107	0.950	0.934	0.975	1.041	0.951	1.073	0.946	1.100	0.948	1.136	0.966
		Mean error	11.36%	8.68%	14.91%	20.17%	10.61%	11.71%	9.89%	10.05%	11.08%	8.88%	13.56%	8.81%

Table 6. Comparison of 85% of ultimate moment and corresponding curvature in descending portion

Beam	Experimental		Cusson		GRK		Razvi		Mendis		Legeron		Weena	
	85% of Ultimate Moment and Corresponding Curvature in ascending portion (ana./exp.)													
	$M_{0.85,d}$ (kN-m)	$\phi_{0.85,d}$ ($\times 10^{-6}$)	$\frac{M_{0.85d,ana}}{M_{0.85d,exp}}$	$\frac{\phi_{0.85d,ana}}{\phi_{0.85d,exp}}$	$\frac{M_{0.85d,ana}}{M_{0.85d,exp}}$	$\frac{\phi_{0.85d,ana}}{\phi_{0.85d,exp}}$	$\frac{M_{0.85d,ana}}{M_{0.85d,exp}}$	$\frac{\phi_{0.85d,ana}}{\phi_{0.85d,exp}}$	$\frac{M_{0.85d,ana}}{M_{0.85d,exp}}$	$\frac{\phi_{0.85d,ana}}{\phi_{0.85d,exp}}$	$\frac{M_{0.85d,ana}}{M_{0.85d,exp}}$	$\frac{\phi_{0.85d,ana}}{\phi_{0.85d,exp}}$	$\frac{M_{0.85d,ana}}{M_{0.85d,exp}}$	$\frac{\phi_{0.85d,ana}}{\phi_{0.85d,exp}}$
U1	15.61	203.96	0.915	1.186	1.117	1.041	1.130	1.014	1.056	1.051	0.973	0.870	1.094	1.047
O1	36.03	88.70	1.066	0.823	1.402	1.174	1.125	1.158	1.120	1.076	1.175	0.910	1.254	1.033
U2	20.82	273.60	0.909	0.603	1.341	0.805	1.218	0.828	1.232	0.854	0.878	0.605	1.001	0.746
O2	35.63	125.05	0.810	0.880	1.295	0.974	1.103	1.113	1.159	1.059	0.957	0.918	1.122	0.960
U3	22.55	142.88	0.968	0.964	1.185	0.813	1.161	0.582	1.088	0.824	1.037	0.770	1.167	0.804
O3	40.17	57.67	0.971	1.080	1.318	1.230	0.939	1.211	0.968	1.204	1.098	1.135	1.207	1.202
		Average	0.940	0.923	1.276	1.006	1.113	0.984	1.104	1.011	1.020	0.868	1.141	0.965
		Mean error	8.22%	16.58%	27.63%	14.22%	13.30%	18.08%	11.43%	11.86%	8.35%	17.71%	14.08%	12.86%

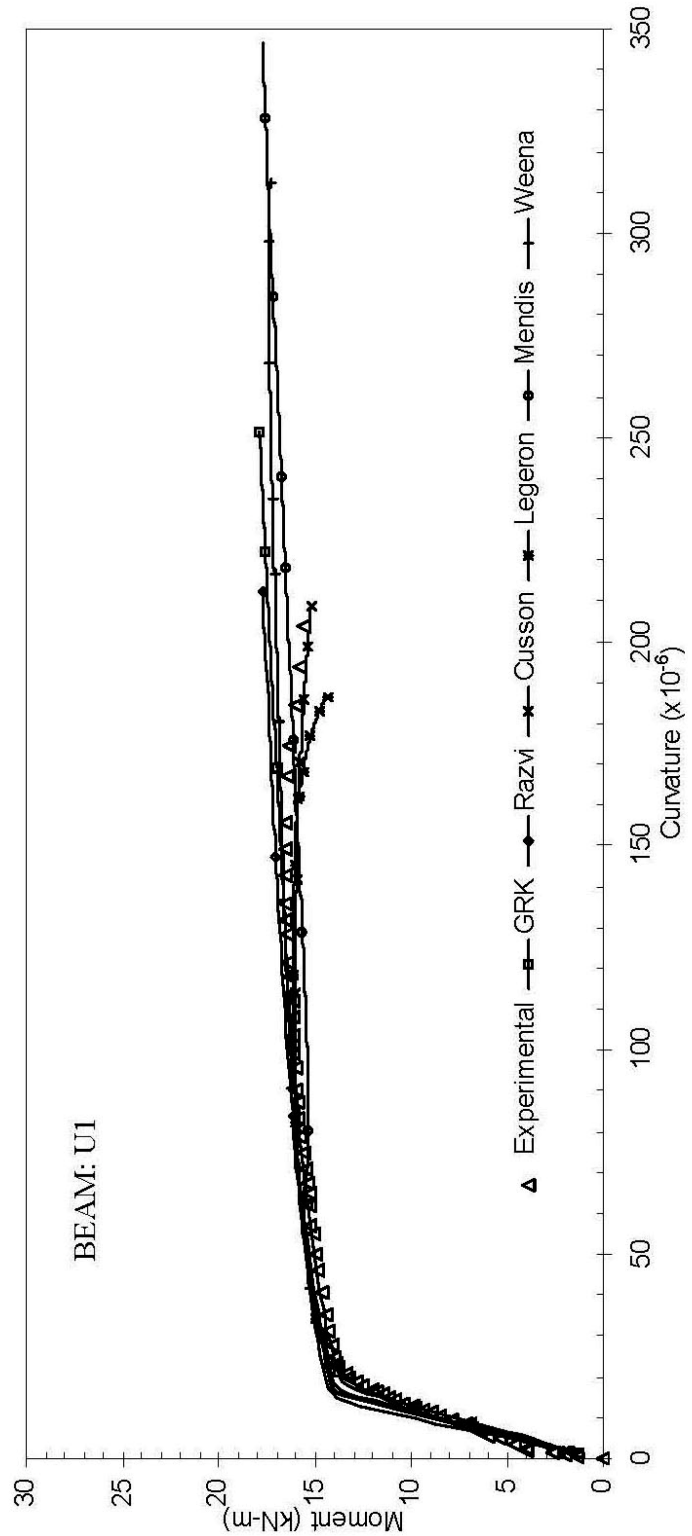
BEAM: U1
Experimental
GRK
Razvi
Cusson
Legeron
Mendis
Weena
Moment (kN-m)
Curvature (x10^{-6})
0
5
10
15
20
25
30
0
50
100
150
200
250
300
350

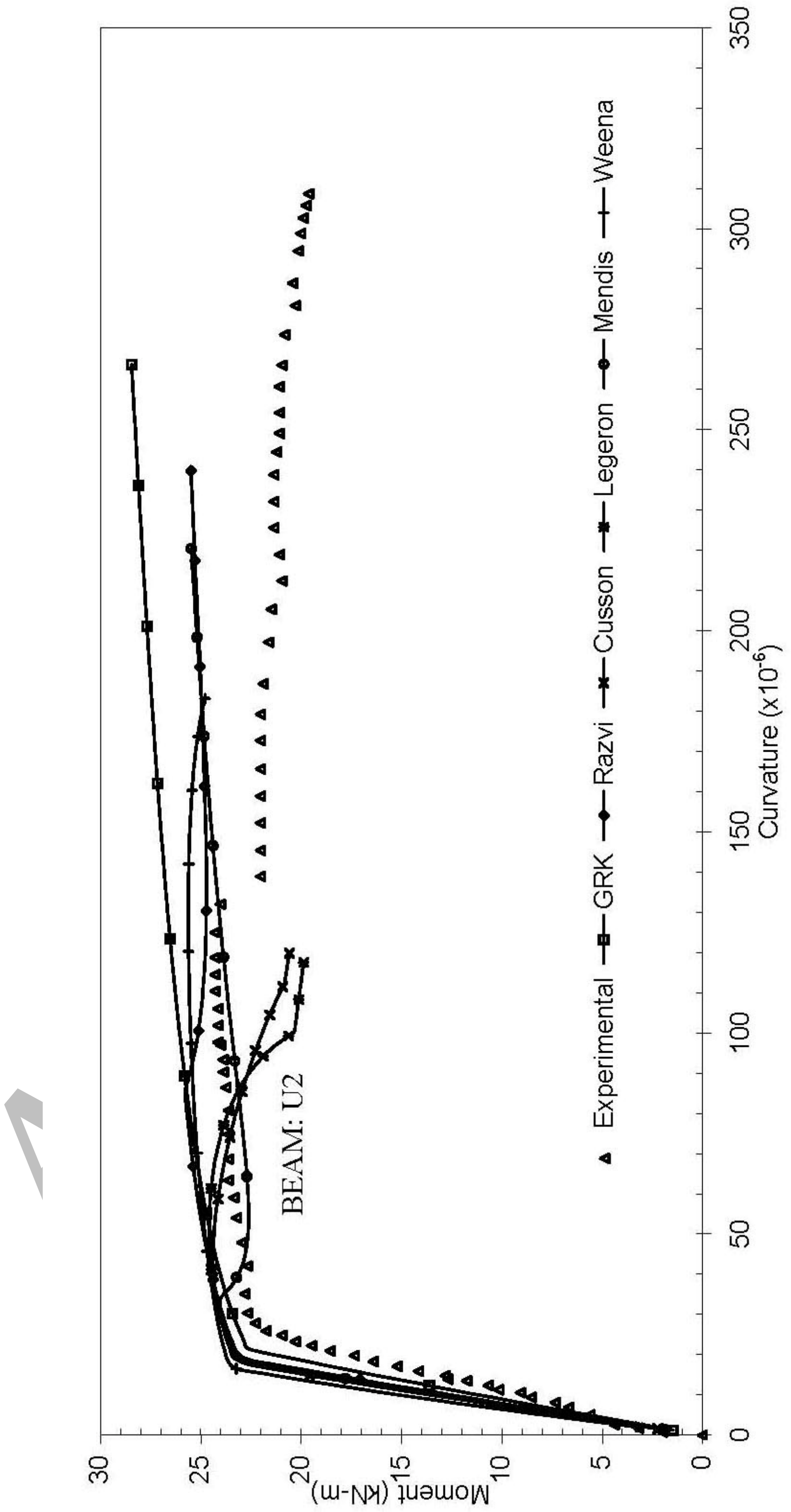

BEAM: U2
Moment (kN-m)
Curvature (x10^-6)
Experimental
GRK
Razvi
Cusson
Legeron
Mendis
Weena
0
5
10
15
20
25
30
0
50
100
150
200
250
300
350

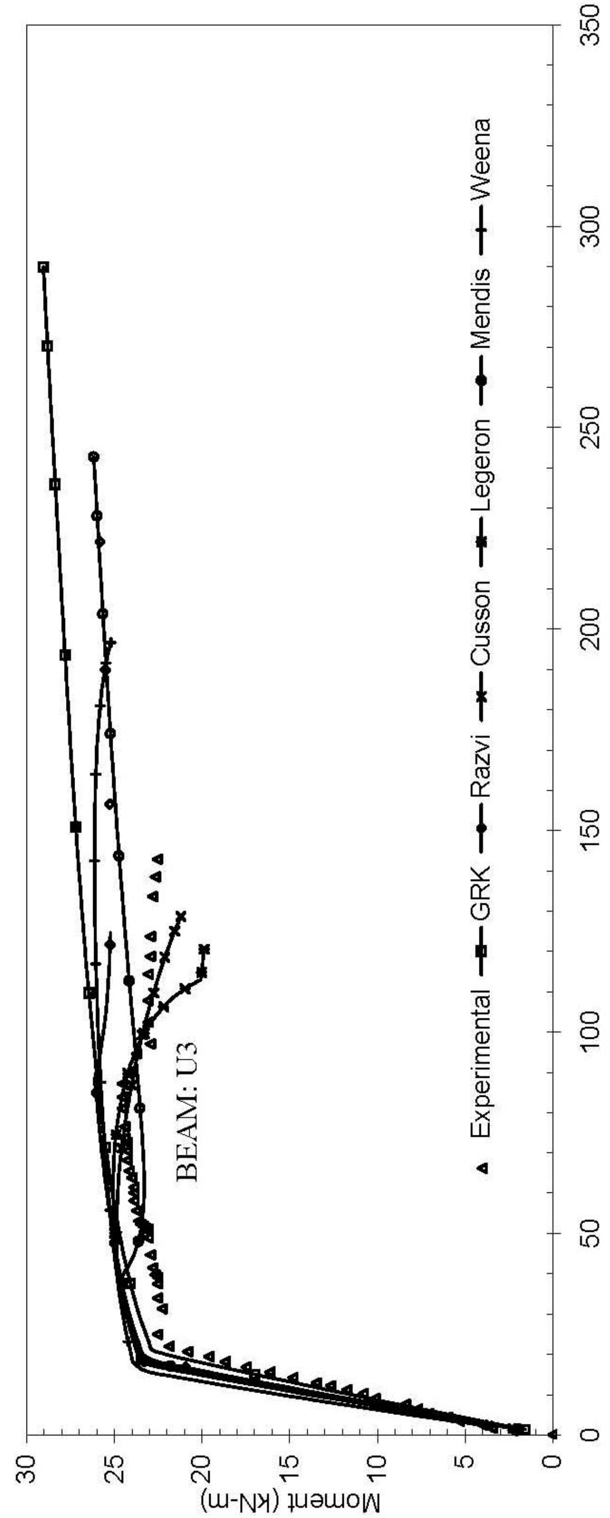

Figure 3. will appear in this page Graphical comparison of analytical and experimental moment ~ curvature curve of over-reinforced beams

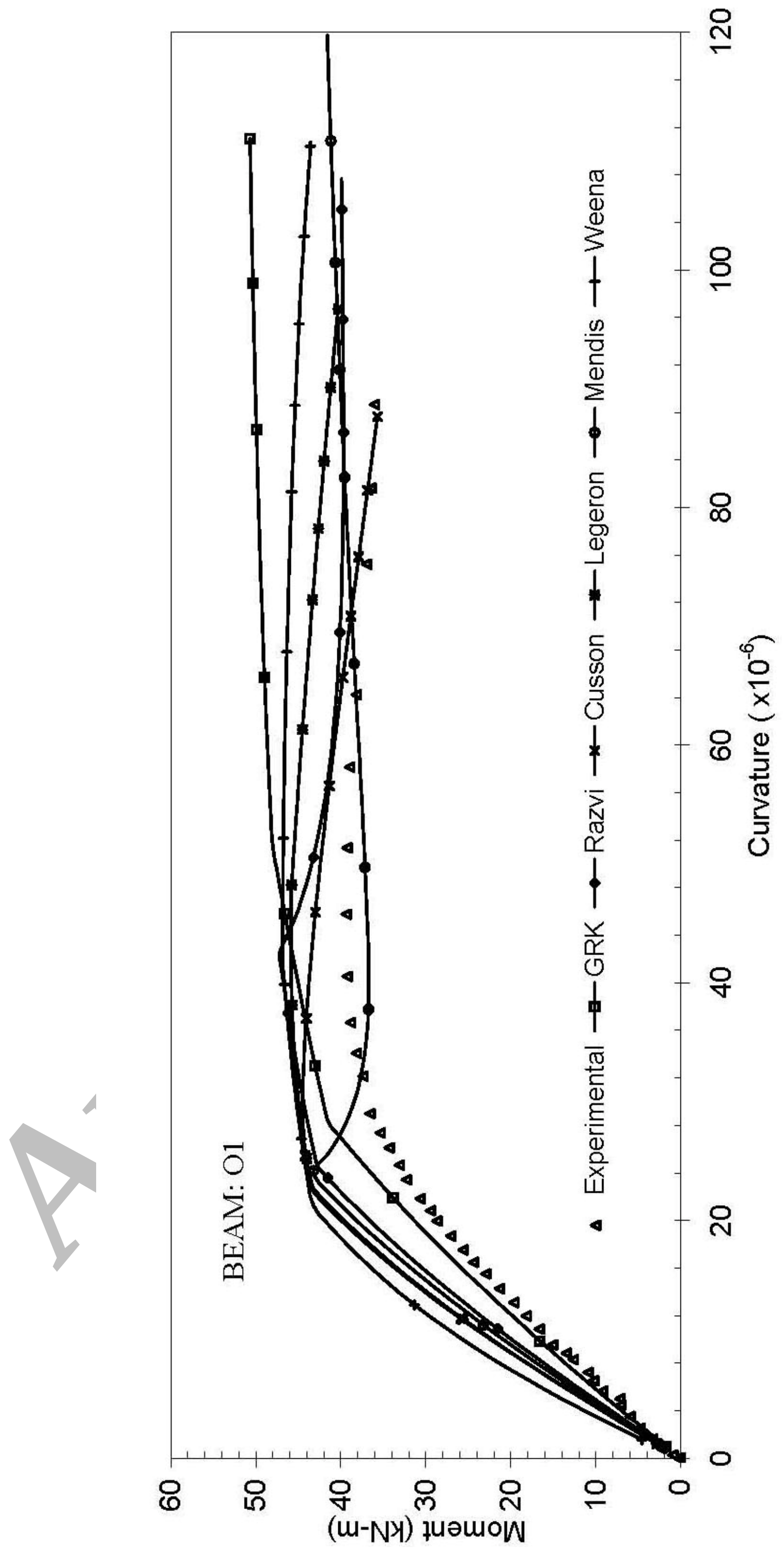
BEAM: O1
Experimental
GRK
Razvi
Cusson
Legeron
Mendis
Weena
Curvature (x10-6)
Moment (kN-m)
0
20
40
60
80
100
120
0
10
20
30
40
50
60

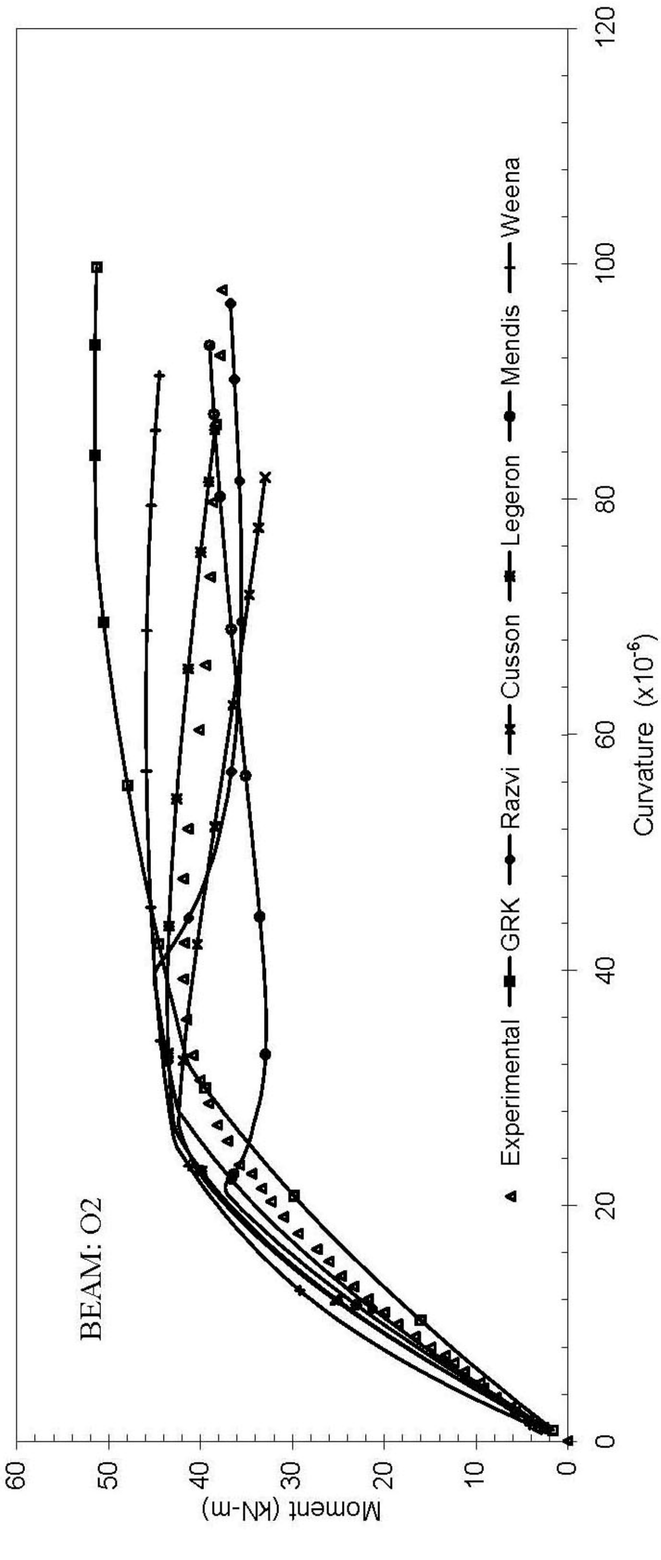
BEAM: O2
Moment (kN-m)
Curvature (x10^{-6})
Experimental
GRK
Razvi
Cusson
Legeron
Mendis
Weena
0
10
20
30
40
50
60
0
20
40
60
80
100
120

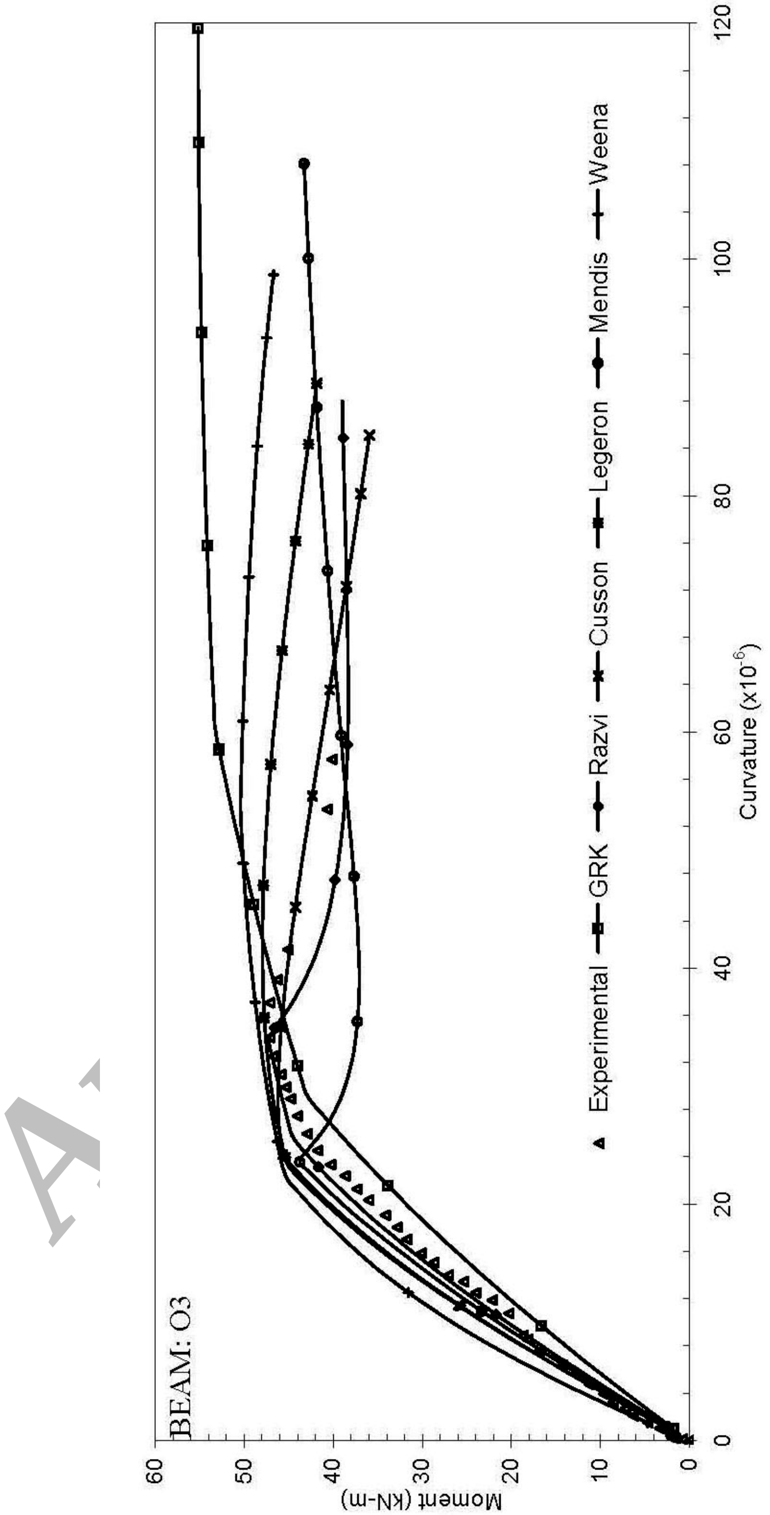

Figure 3. will appear in this page Graphical comparison of analytical and experimental moment ~ curvature curve of over-reinforced beams

NOTATIONS

b	Width of beam
D	Overall depth of beam
d	Effective depth of beam
nd	Depth of Neutral Axis (NA)
ε_c	Extreme compression fiber strain
ε_s	Strain in steel
γ	Reduction factors for distance between CG from NA
α	Reduction factors for area under stress-strain curve respectively
C_c	Compressive force
f_{ck}	Concrete characteristics compressive strength
s	Tie spacing
f_y	Yield strength of reinforcement steel
M	Moment
ϕ	Curvature
T	Total tensile force in tensile steel
C_s	Compressive force in compression steel
M_t	Moment of force in tensile steel about the N.A.
M_c	Moment of compressive force in concrete about the N.A.
M_{cs}	Moment of force in compression steel about the N.A.
M_u	Ultimate moment
ϕ_u	Curvature corressponding to the ultimate moment
$M_{0.85,a}$	85 % of the ultimate moment in ascending portion
$\phi_{0.85,a}$	Curvature corresponding to 85 % of the ultimate moment in ascending portion
$M_{0.85,d}$	85% of the ultimate moment in descending portion
$\phi_{0.85,d}$	Curvature corresponding to 85% of the ultimate moment in descending portion
$M_{u,ana}$	Analytical ultimate moment
$M_{u,\exp}$	Experimental ultimate moment
$\phi_{u,ana}$	Analytical curvature corresponding to ultimate moment
$\phi_{u,\exp}$	Experimental curvature corresponding to ultimate moment
$M_{0.85a,ana}$	Analytical 85% of ultimate moment in ascending portion
$M_{0.85a,\exp}$	Experimental 85% of ultimate moment in ascending portion
$\phi_{0.85a,ana}$	Analytical curvature corresponding to 85% of ultimate moment in ascending portion
$\phi_{0.85a,\exp}$	Experimental curvature corresponding to 85% of ultimate moment in ascending portion
$M_{0.85d,ana}$	Analytical 85% of ultimate moment in descending portion
$M_{0.85d,\exp}$	Experimental 85% of ultimate moment in descending portion
$\phi_{0.85d,ana}$	Analytical curvature corresponding to 85% of ultimate moment in descending portion

$\phi_{0.85d,\exp}$ Experimental curvature corresponding to 85% of ultimate moment in descending portion

REFERENCES

1. Cheong, H.K., and Hong Zeng, Stress-strain relationship for concrete confined by lateral steel reinforcement, *ACI Materials Journal*, May-June, No. 3, **99**(2002) 250-255.
2. Cusson, D., and Paultre, P., Stress-strain model for confined high-strength concrete, *Journal of Structural Engineering, ASCE*, No 3, **121**(1995) 468-477.
3. Han, B.S., Shin, S.W., and Bahn, B.Y., A model of confined concrete in high strength reinforced concrete tied columns, *Magazine of Concrete Research*, No. 3, **33**(2003) 203-214.
4. Konstantinidis, D., and Kappos, A.J., Analytical modeling of confined HSC columns under flexure and axial load, *Magazine of Concrete Research*, No. 4, **55**(2003) 395-403.
5. Kumar, G. Rajesh and Rao, A.K., Strength and deformability characteristics of tie confined standard concrete. *Journal of Indian Concrete Institute*, October-December, No. 3, **6**(2005) 19-25.
6. Frederic, L., and Paultre, P., Uniaxial confinement model for normal and high strength concrete columns, *ASCE Journal of Structural Engineering*, No. 2, **129**(2003) 241-252.
7. Mendis, P., Pendyala, R., and Setunge, S., Stress Strain Model to Predict the Full Range Moment Curvature Behaviour of High Strength concrete Sections, *Magazine of Concrete Research*, No. 4, **52**(2000) 227-234.
8. Serna Ros, P., Yazzar, S.A., and Coca Calvo, A., Influence of Confinement on High Strength Concrete Behavior, *Materials and Structures, RILEM Publications*, **36**(2003) 439-447.
9. Park, R. and Paulay, T., *Reinforced Concrete Structures*. Wiley-Inter-Science, **6**(1975) 196-268.
10. Paultre, P., Legeron, F., and Mongeou, D., Influence of concrete strength and transverse reinforcement yield strength on behaviour of high strength concrete columns, *ACI Structural Journal*, July-August, No. 4, **98**(2001) 490-501.
11. Razvi, S., and Saatcioglu, M., Confinement model for high-strength concrete, *Journal of Structural Engineering, ASCE*, No 3, **125**(1999) 281-289.
12. Sharma, U., Bhargava, P., and Kaushik, S.K., Comparative Study of Confinement Models for High-Strength Concrete Columns, *Magazine of Concrete Research*, No. 4, **57**(2005) 185-197.
13. Weena, P.L., Sanjayan, J.G., and Setunge, S., Stress-strain model for laterally confined concrete, *Journal of Materials in Civil Engineering*, No. 6, **17**(2005) 607-616.
14. IS:383, Specification for coarse and fine aggregate from Natural Sources for Concrete. Bureau of Indian Standards, 1970.
15. IS:456, Code of practice for plain and reinforced concrete. Bureau of Indian Standards, 2000.
16. IS: 12269, Specification for 53 Grade Ordinary Portland Cement. Bureau of Indian Standards, 1987.